

**Supporting Information for “Hybrid nanostructure of  
platinum-nanoparticles/graphitic-nanofibers as a three-dimensional  
counter electrode in dye-sensitized solar cells “**

Chien-Kuo Hsieh,<sup>a</sup> Ming-Chi Tsai,<sup>a</sup> Ching-Yuan Su,<sup>a</sup> Sung-Yen Wei,<sup>a</sup> Ming-Yu  
Yen,<sup>b</sup> Chen-Chi M. Ma,<sup>b</sup> Fu-Rong Chen,<sup>a</sup> and Chuen-Horng Tsai <sup>\*a</sup>

<sup>a</sup> *Department of Engineering and System Science, National Tsing Hua University,  
Hsinchu 30013, Taiwan, R.O.C.*

<sup>b</sup> *Department of Chemical Engineering, National Tsing Hua University, Hsinchu  
30013, Taiwan, R.O.C.*

\*E-mail: [chtsai@ess.nthu.edu.tw](mailto:chtsai@ess.nthu.edu.tw)

## 1. Schematic diagram of the fabrication flow for PtNPs/GNFs hybrid nanostructure 3D counter electrode

Ni film was deposited on FTO conductive substrate for GNFs growth, the area and thickness were  $0.28\text{cm}^2$  and  $10\text{nm}$ , respectively. The Ni catalyst deposited FTO glass was then placed on a quartz plate and loaded into furnace quartz tube to grow the homogenous and high-density GNFs at  $530^\circ\text{C}$ , FTO glass still kept the electrical conductivity without compromising at this low temperature LPCVD process. After that, the specimen underwent hydrophilic treatment and then electrodeposited PtNPs subsequently.

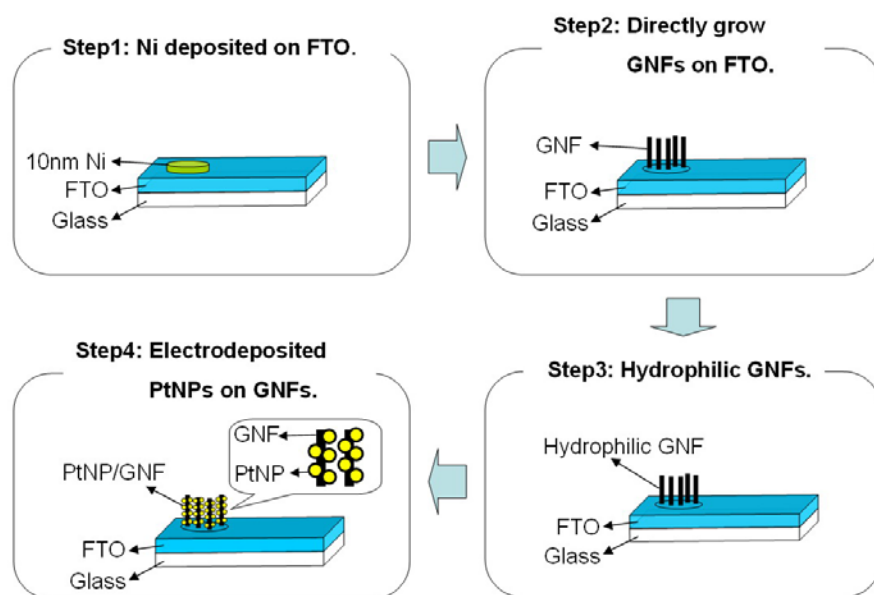


Figure S1. Fabrication flow of PtNPs/GNFs hybrid nanostructure 3D counter electrode.



Figure S2. A photography of our direct growth of GNFs on FTO glass.

## 2. GNFs hydrophilic treatment

The hydrophilic treatment was performed at  $50 \text{ mV s}^{-1}$  for 50 cycles, with a potential ranging from  $-0.25 \text{ V}_{\text{SCE}}$  to  $+1.25 \text{ V}_{\text{SCE}}$  (potential versus saturated calomel electrode), in an  $\text{O}_2$ -saturated  $0.5 \text{ M H}_2\text{SO}_4$  aqueous solution.

## 3. PtNPs electrodeposited on hydrophilic GNFs

The hydrophilic GNF/FTO was subjected to electrodeposition in a plating bath containing an  $\text{N}_2$ -saturated Pt precursor aqueous solution ( $0.5 \text{ mM H}_2\text{PtCl}_6 \cdot 6\text{H}_2\text{O}$  and  $0.15 \text{ M C}_6\text{H}_8\text{O}_7 \cdot \text{H}_2\text{O}$  in DI water). In each scan, voltages of  $0 \text{ V}_{\text{SCE}}$  and  $-1.25 \text{ V}_{\text{SCE}}$  were applied for durations of 2.5 sec and 0.2 sec, respectively. 100 scans were used to deposit the PtNPs on the GNFs. The PtNP/GNF hybrid counter electrode was then rinsed with DI water, and subsequently baked under vacuum at  $250^\circ\text{C}$  in order to remove moisture.

The hydrophilic treatment of the GNFs and the electrodeposition of the PtNPs were performed using a potentiostat/galvanostat (PGSAT 302N, Autolab, EcoChemie) in a three-electrode configuration, at a controlled temperature of  $30^\circ\text{C}$  under ambient pressure. A Pt-coated Ti mesh and a saturated calomel electrode were used as the counter and reference electrode, respectively.

## 4. Working electrode preparation

The working electrode utilized the same FTO glass (TEC-7, 2.2 mm, Hartford) coated with nanocrystalline  $\text{TiO}_2$  (the coating was performed using print-screen technology); the area and thickness of the  $\text{TiO}_2$  film were about  $0.28 \text{ cm}^2$  and  $10 \mu\text{m}$ , respectively. After printing, the working electrodes were dried at  $125^\circ\text{C}$ , then sintered in air at  $500^\circ\text{C}$  for 30 min. Prior to the fabrication of the DSSCs, the sintered working electrodes were immersed in a N719 (Solaronix) solution ( $0.3 \text{ mM}$  in a mixture of

acetonitrile and tert-butylalcohol [volume ratio 1:1]) at room temperature for 24 hr. The dye-adsorbed electrode was then washed with acetonitrile and dried.

## 5. DSSCs fabrication and photovoltaic performance measurement

A 60  $\mu\text{m}$ -thick hot melt spacer (SX1170-60, Solaronix) was sandwiched between the sensitized  $\text{TiO}_2$  working electrode and various counter electrodes by heating at  $100^\circ\text{C}$  for a few seconds. The spacer between the electrodes was injected with a liquid, iodide-based electrolyte (AN-50, Solaronix). The photocurrent voltage characteristics of the DSSC devices were measured under simulated solar illumination (AM 1.5,  $100 \text{ mW}/\text{cm}^2$ , Oriel 91160), at  $25^\circ\text{C}$ . The solar light was calibrated using a reference Si cell (calibrated at NREL, PVM-81).

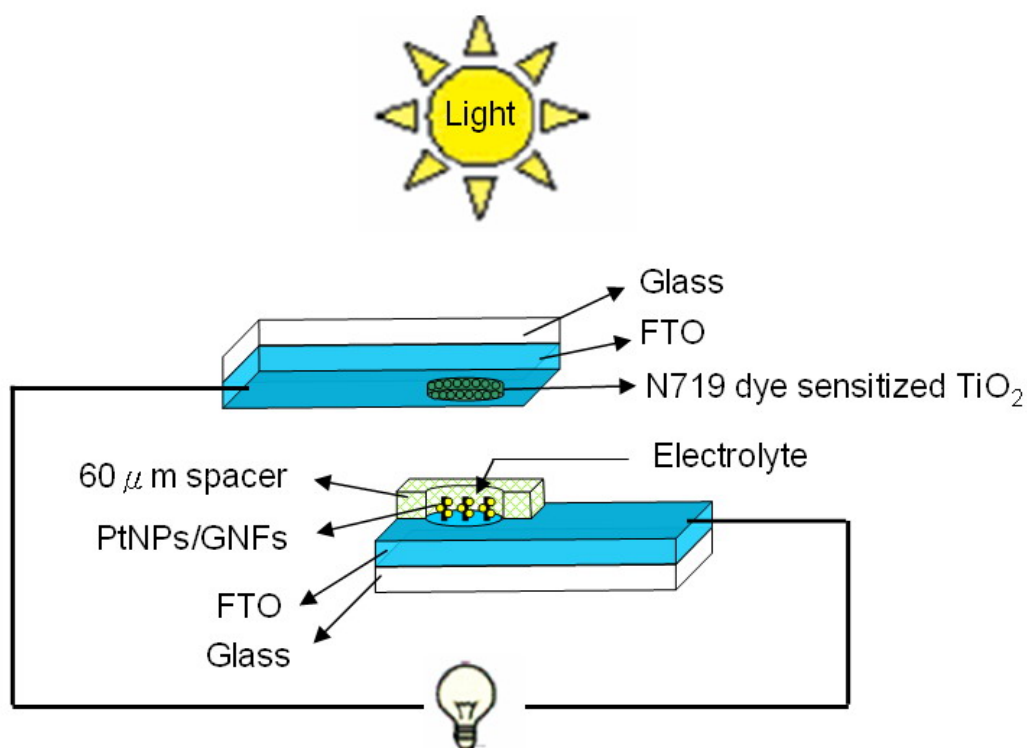


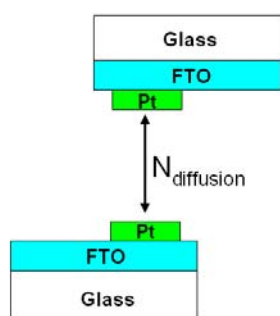
Figure S3. Schematic diagram of the DSSCs.

## 6. Fitting model and parameters definitions for equivalent circuits.

Figure S4 shows the schematic diagram of the symmetric configuration for EIS measurement. Figure S4 (a) shows the two-dimensional (2D) plane structure electrode, the electrolyte diffuse between the 2 electrodes and  $N_{\text{diffusion}}$  can be obtained, this is a long-distance diffusion. Figure S4 (b) shows the electrolyte diffusion in the three-dimensional (3D) porous structure electrode. The size of  $I_3^-$  ion is 3 Å in diameter and 5.8 Å in length<sup>1</sup>, we suggested this small size of  $I_3^-$  ion can easily diffuse through the GNFs forest, and the second  $N_{\text{diffusion}}$  ( $N_{\text{porosity}}$ ) can be obtained, this is a short-distance diffusion within the electrode. Figure S5 (a) and (b) show the impedance spectra at various applied bias, for the 2D plane structure (Pt film) and the 3D porous structure (GNFs forest), respectively. The inserts in the figure S5 are enlarged spectra at the high frequency scan range. As we can see, compared with the conventional Pt film (2D plane structure) having 2 semi-circles, the GNFs forest (3D porous structure) shows 3 semi-circles. With increased bias, a small semi-circle showing a constant behavior at the high frequency scan range in the GNFs forest electrode was observed and shown in Figure S5 (b). This evidence suggested that the typical equivalent circuit of Pt film may not be appropriate for our system. Figure S6 (a) shows the fitting model and parameter definitions of a typical equivalent circuit for the 2D plane structure (Pt film). Based on the EIS result, we suggested the modificatory equivalent circuit for the 3D porous structure (GNFs forest) which is shown in Figure S6 (b). The first semi-circle at high-frequency is attributed to the second Nerest diffusion impedance resulting from the short-distance diffusion within the electrode ( $N_{\text{porosity}}$ ), the second semi-circle represents the charge-transfer resistance and capacitance of the catalyst/electrolyte interface ( $R_{\text{ct}}$  and CPE), the third semi-circle at low-frequency scan range is the long-distance Nerest diffusion between the electrodes ( $N_{\text{diffusion}}$ ). Some simulation investigations reported the influence on

electrode roughness and porosity<sup>2,3</sup>. Recently, Joseph *et al.* who reported similar result as our experimental data<sup>4</sup>, our data support the second Nernst diffusion impedance which was attributed to the porosity of the GNFs forest.

(a). 2D electrode: plane structure.



(b). 3D electrode: porous structure.

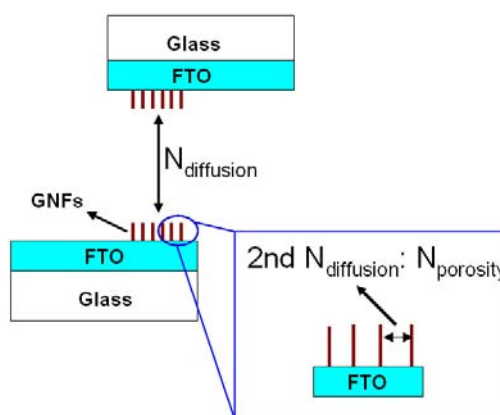


Figure S4. Schematic of (a) 2D plane structure, and (b) 3D porous structure electrode.

The  $N_{\text{diffusion}}$  is attributed to a long-distance diffusion between the electrodes; the

$N_{\text{porosity}}$  is attributed to a short-distance diffusion within the electrode.

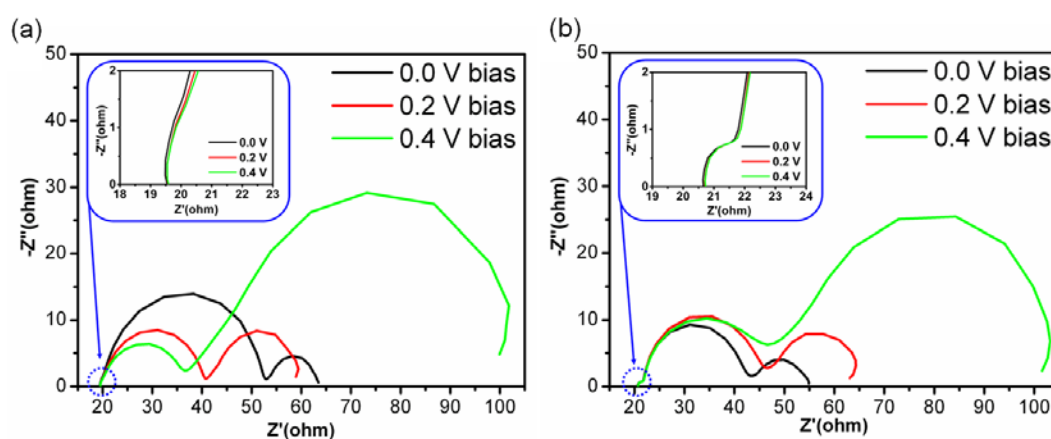


Figure S5. Impedance spectra for symmetric cell at various applied bias. (a) 2D plane structure (Pt film). (b) 3D porous structure (GNFs forest). The inserts are enlarged spectra at the high frequency scan range.

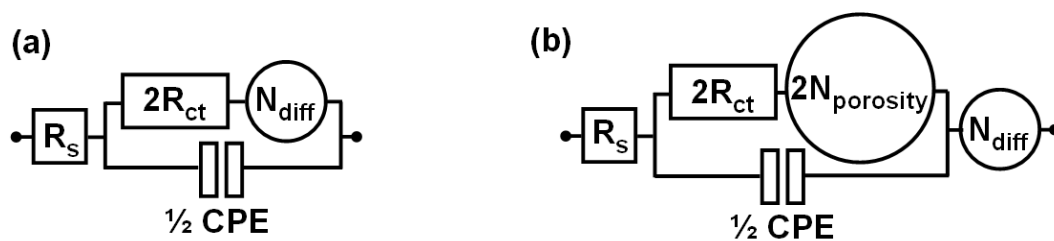


Figure S6. The fitting model and parameter definitions of (a) the typical equivalent circuit for the 2D plane structure (Pt film), and (b) modificatory equivalent circuit for the 3D porous structure (GNFs forest).

## 7. Efficiency improvement comparison of various hybrid PtNPs/carbon nanomaterials

Table S1 shows the efficiency improvement comparison of hybrid PtNPs/carbon nanomaterials as a counter electrode in DSSCs, including PtNPs/CB <sup>5</sup>, PtNPs/MC <sup>6</sup>, PtNPs/MWCNT <sup>7</sup> and our PtNPs/GNF. As we can in the Table S1, compared with the traditional Pt film, the hybrid PtNPs/GNFs nanostructure show the highest efficiency improvement up to 17.82 %.

Literature	Counter Electrode	J <sub>sc</sub> (mA/cm <sup>2</sup> )	V <sub>oc</sub> (V)	F.F.	η (%)	η improve (%)	Journal & Year
a	Pt	14.86	0.72	0.61	6.63	0.75	Solar Energy, 2009 <sup>5</sup>
	PtNPs/CB	14.73	0.74	0.61	6.68		
b	Pt	17.52	0.61	0.60	6.42	3.27	IJP, 2010 <sup>6</sup>
	PtNPs/MC	17.11	0.63	0.61	6.63		
c	Pt	14.62	0.74	0.64	6.92	15.61	JMC, 2010 <sup>7</sup>
	PtNPs/MWCNT	18.01	0.73	0.61	8.00		
	Pt	12.83	0.69	0.60	5.22	17.82	Our data
	PtNPs/GNF	13.67	0.70	0.64	6.15		

Table S1. Summary of efficiency improvement for hybrid Pt/carbon nanomaterials as a counter electrode in DSSCs. CB: Carbon Black, MC: Mesoporous Carbon, MWCNT: Multi Wall Carbon Nanotube, GNF: Graphite Nanofiber.

## 8. EDX analysis.

Figure S7 to Figure S9 show the EDX analysis, for FTO glass, GNFs on FTO glass, and PtNPs/GNFs on FTO glass, respectively. Figure S7 shows the EDX of FTO glass, the peaks consists tin (Sn), silicon (Si) and oxygen (O). Figure S8 shows the EDX of GNFs on FTO glass, the peaks consists Sn, Si, O, nickel (Ni) and carbon (C), the weak Ni peak is attributed to the catalyst layer for GNFs growth. Figure S9 shows the EDX of PtNPs/GNFs on FTO glass, the peaks consists Sn, O, C, and platinum (Pt), the strong Pt peak is attributed to the PtNPs deposited on the GNFs.

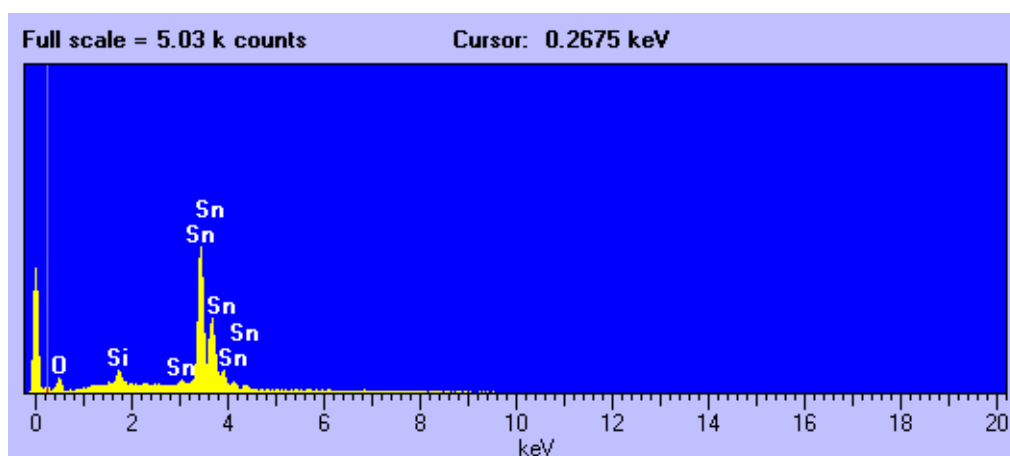


Figure S7. EDX of FTO glass.

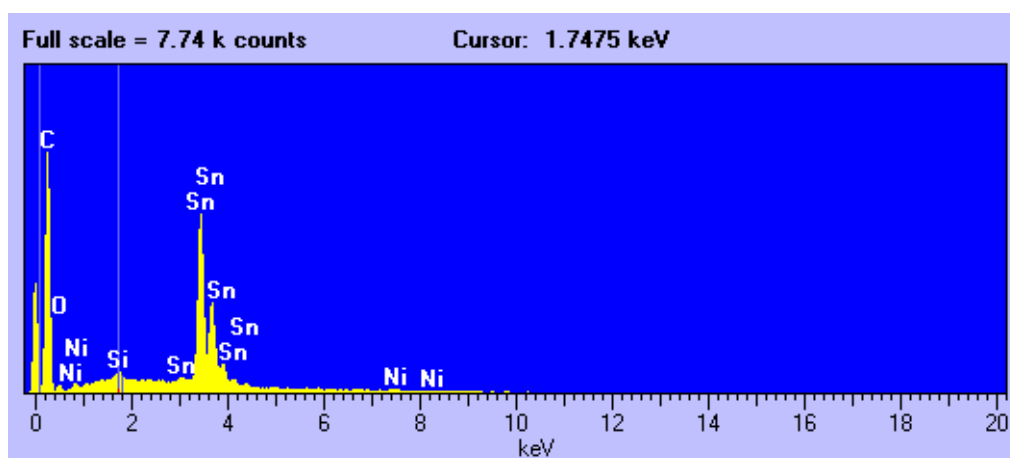


Figure S8. EDX of GNFs on FTO glass.

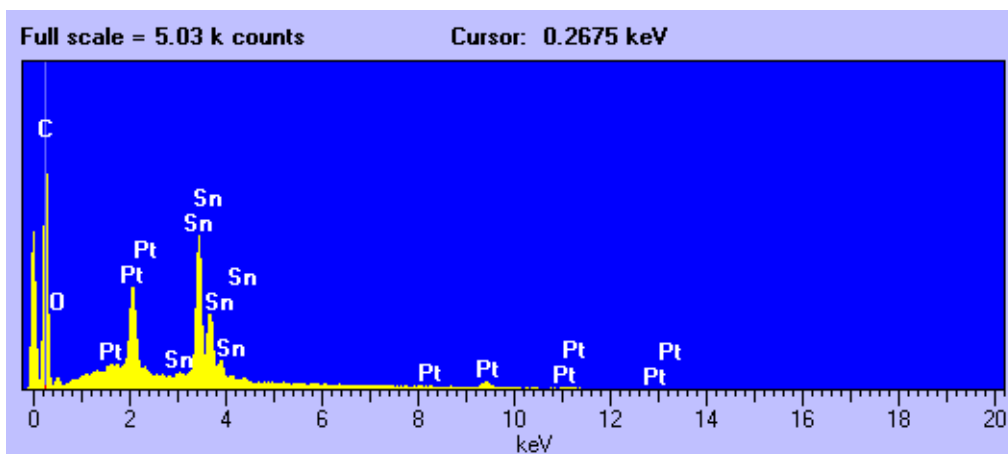


Figure S9. EDX of Pt/GNFs on FTO glass.

## Reference

1. H. Sakane, T. Mitsui, H. Tanida and I. Watanabe, *J. Synchrot. Radiat.*, 2001, **8**, 674.
2. D. Menshykau and R. G. Compton, *Electroanalysis*, 2008, **20**, 2387.
3. D. Menshykau and R. G. Compton, *J. Phys. Chem. C*, 2009, **113**, 15602.
4. J. D. Roy-Mayhew, D. J. Bozym, C. Punckt and I. A. Aksay, *Acs Nano*, 2010, **4**, 6203.
5. P. J. Li, J. H. Wu, J. M. Lin, M. L. Huang, Y. F. Huang and Q. G. Li, *Sol. Energy*, 2009, **83**, 845.
6. G. Q. Wang, J. F. Gu and S. P. Zhuo, *Int. J. Photoenergy*, 2010, 389182.
7. K. C. Huang, Y. C. Wang, R. X. Dong, W. C. Tsai, K. W. Tsai, C. C. Wang, Y. H. Chen, R. Vittal, J. J. Lin and K. C. Ho, *J. Mater. Chem.*, 2010, **20**, 4067.